Nucleic Acids Research, 1998, Vol. 26, No. 21 **4811–4817**

Suppression of electrophoretic anomaly of bent DNA segments by the structural property that causes rapid migration

Takashi Ohyama*, Hiromi Tsujibayashi, Hideki Tagashira, Koichi Inano[1], Takayuki Ueda[2], Yoshiko Hirota[3] and Koichiro Hashimoto[3]

Department of Biology, Faculty of Science, Konan University, 8-9-1 Okamoto, Higashinada-ku, Kobe 658, Japan, [1]Department of Laboratory Medicine, Niigata University School of Medicine, 1-757 Asahimachi, Niigata 951, Japan, [2]Research Laboratory for Molecular Genetics, Niigata University, 1-757 Asahimachi, Niigata 951, Japan and [3]Meiji Institute of Health Science, 540 Naruda, Odawara 250, Japan

Received August 7, 1998; Revised and Accepted September 22, 1998 DDBJ/EMBL/GenBank accession nos AB010555 and AB010556

ABSTRACT

Intrinsic DNA curvature is speculated to be a common feature of all satellite DNA sequences and may aid in the tight winding of DNA in constitutive heterochromatin. Several satellite DNAs, however, show unusually rapid migration in non-denaturing polyacrylamide gels, which is just the opposite behavior of that shown by curved DNA structures. Employing bovine satellite I DNA monomer, we attempted to understand the molecular mechanism of 'rapid migration'. The phenomenon of rapid migration was temperature-dependent and to a small extent polyacrylamide-concentration-dependent. Physiological or near-physiological concentrations of Mg^{2+} and Ca^{2+} ions bent the rapid migrating DNA segment. Predominance of purine–purine base stacking over purine–pyrimidine in nucleotide sequence was strongly indicated to be the cause of the rapid migration. Furthermore, they seemed to be implicated in the formation of induced DNA bend. We also found that the satellite I monomer contains an intrinsic DNA curvature as do many other satellites. Heretofore, the rapid migration property has concealed the presence of curvature.

INTRODUCTION

Eukaryotic genomes contain tandemly repeated DNA sequences known as satellites (1,2). Satellites comprise anywhere from a few percent to >50% of mammalian genomes (2). Although satellites are universally associated with regions of constitutive heterochromatin, no common structural features are known to be shared by all satellites. The unit DNA sequences of satellites show enormous variation in length, sequence and nucleotide composition. Intrinsically bent DNA structures have been suggested to function in the folding of DNA into chromosomes (3–5), and several findings of bent satellite DNAs (6–8) have raised an attractive possibility that intrinsic DNA curvature may be a common feature of all satellites. DNA curvature may aid in the tight winding of DNA in constitutive heterochromatin.

Martínez-Balbás *et al.* (9) analyzed 20 different satellite DNA sequences and concluded that, in satellite DNA, adenine residues show a high tendency to cluster in groups of three or more, which raised the possibility that all the satellites that they examined contained a curved DNA structure. Indeed, they showed experimentally that mouse, rat and α-monkey satellite DNA monomers each contain a curved DNA structure. They did not, however, report on whether the tracts in the rest of the satellite sequences were present in a periodicity that forms curved DNA structure. Fitzgerald *et al.* (10) employed an electrophoretic method and computer analysis and reported that a conserved sequence pattern of bending was seen in all 57 satellite sequences that they examined. However, in their study, several repeated sequences did not show the retarded migration in non-denaturing polyacrylamide gels that is characteristic of curved DNA fragments. Strongly bent sequences constituted less than half of the satellites they examined. Furthermore, (G+C)-rich satellite sequences of box turtle (*Terrapene carolina*), Komodo dragon (*Varanus komodoensis*), vulture (*Cathartes aura*) and cow (*Bos taurus*) migrated unusually rapidly. It is probable that some property of DNA which causes the rapid migration behavior may conceal the presence of a curved DNA structure in gel electrophoresis.

In addition to the above report, rapid migration behavior is reported for (A+T)-rich fragments from yeast centromeres (11). Milot *et al.* (12) also found such fragments in a study of illegitimate chromosomal recombination in mammalian cells. An analysis of the molecular basis for the rapid migration of DNA fragments may reveal more about the universality of bent satellite DNA and help in studying the structural requirements for several distinctive regions in eukaryotic genomes.

This study attempts to understand the molecular mechanism of the rapid migration behavior of DNA fragments. We resolved a digest of bovine genomic DNA, cloned and sequenced the repetitive sequences that showed such behavior. One half of the repeating unit of bovine satellite I DNA was found to migrate unusually rapidly in non-denaturing polyacrylamide gels. The other half contained an intrinsic DNA curvature, as do many other satellites, but

*To whom correspondence should be addressed. Tel/Fax: +81 78 435 2547; Email: ohyama@base2.ipc.konan-u.ac.jp

electrophoretic anomaly caused by the structure was suppressed by the rapid migration property of the fragment. The phenomenon of rapid migration was temperature-dependent. Polyacrylamide concentration in a gel also influenced their mobilities. Interestingly, physiological or near-physiological concentrations of Mg^{2+} and Ca^{2+} ions bent the rapid-migrating DNA segment. Predominance (>80%) of purine–purine (or pyrimidine–pyrimidine) base stacking over purine–pyrimidine (or pyrimidine–purine) throughout the entire satellite I sequence seemed to be the cause of the rapid migration. This study presents the results of the first systematic study to understand the molecular basis of rapid migration.

MATERIALS AND METHODS

Two-dimensional gel electrophoresis and cloning of DNA fragments

The procedure for the two-dimensional (2D) gel electrophoresis was similar to that described before (13). Briefly, the *Pst*I digest (0.4 µg) of bovine (*B.taurus*) genomic DNA (purchased from Toyobo, Tokyo) was subjected to 2D gel electrophoresis carried out in 1/2 × TBE (45 mM Tris–borate/1 mM EDTA, pH 8.3). The sample was run in the first dimension on a 1.0% agarose tube gel (0.25 cm × 13 cm) at room temperature and constant voltage. Then, the gel was removed from the glass tube and placed onto a 7.5% polyacrylamide slab gel (0.1 cm × 14 cm × 13 cm; acrylamide:bisacrylamide = 29:1). Electrophoresis was carried out at constant voltage at 4°C and the gel was stained with ethidium bromide. Then, two spots of interest (indicated by F and N in Fig. 2) were excised from the gel. The DNA fragments in the spots were electroeluted and cloned into the *Pst*I site of plasmid pUC19.

Measurement of electrophoretic mobility

The construct carrying the F fragment and that carrying the N fragment were digested with *Pst*I. Each digest was extracted with phenol, precipitated with ethanol, rinsed with 70% ethanol and dried. Temperature-dependence of the mobility was investigated by using 7.5% non-denaturing polyacrylamide gels (29:1 acrylamide:bis-acrylamide; this ratio was common to all gels described below) that contained 1/2 × TBE (45 mM Tris–borate/1 mM EDTA, pH 8.3). Electrophoresis was carried out in the same buffer at 5, 20, 35 and 50°C. Electrophoretic mobilities of the DNA fragments in 5, 7.5, 10, 12.5 and 15% gels were investigated at 5°C. These gels contained 1/2 × TBE and the electrophoresis was performed in the same buffer. In both experiments, DNA samples were dissolved in TE (10 mM Tris–HCl, pH 7.5; 1 mM EDTA, pH 8.0), mixed with dye solution containing bromophenol blue, xylene cyanol and glycerol (the final concentration of each component was 0.04, 0.04 and 5%, respectively) and loaded onto gel slots.

The mixture of *Hinc*II and *Hae*III digests of phage ϕX174 DNA was used as a source of size marker DNA fragments. Among the fragments, the 1353, 1078, 770, 495, 392, 234, 210, 194 and 162 bp fragments seemed to be 'ordinary' DNA fragments because plotting their data points for the log of each fragment size and its electrophoretic mobility always resulted in smooth lines (almost straight but slightly curved in the high molecular weight region), irrespective of the changes in electrophoretic conditions (temperature, polyacrylamide concentrations and presence of divalent cations). The electric field across the gels was maintained at 2.4 V/cm. After electrophoresis, gels were stained with ethidium bromide.

Circular permutation analysis

A tandem dimer of each of the F, N and *Hae*II–*Pst*I (derived from N) fragments was cloned into *Pst*I (in the case of F and N fragments) or *Sma*I site of plasmid pUC19. Each construct was digested with restriction enzymes as indicated in each corresponding figure. The F- and N-derived permuted fragments were subsequently blunt-ended. DNA digests were purified by phenol extraction and ethanol precipitation. The circular permutation analysis (14) was carried out at 5°C by using 7.5% gels.

The effects of Mg^{2+} or Ca^{2+} ions on mobilities of F- and N-derived permuted fragments were investigated as follows. The gels contained, and the running buffers were comprised of, 1/2 × TB (45 mM Tris–borate, pH 8.3) and 10 mM $MgCl_2$ or $CaCl_2$. In the experiment, sample and marker DNA solutions (~10 µl) each contained 1/2 × TB, the same chloride concentration as that contained in the gel and running buffer, 0.04% bromophenol blue, 0.04% xylene cyanol and 5% glycerol. The buffer solution was pumped between the electrode compartments at a rate of ~1200 ml/h. In addition, each compartment was stirred during electrophoresis.

Nucleotide sequence accession numbers

The nucleotide sequence data reported in this study appear in the DDBJ, EMBL and GenBank nucleotide sequence databases with the accession numbers AB010555 and AB010556.

RESULTS

Repeating unit of bovine satellite I DNA was divided into two segments that showed different electrophoretic behaviors

Bovine satellite I DNA localizes in the centromeres of all of the autosomes (15). The repeating unit of the satellite DNA (*Eco*RI fragment of ~1400 bp; 16) migrates more rapidly than the bulk of the genomic DNA fragments in 2D gel electrophoresis using non-denaturing polyacrylamide gels (10). The unit has two *Pst*I sites: one is located near the 5′ end of the unit and the other near the center. These sites were separated by ~700 bp from each other (Fig. 1). Interestingly, we found that in 2D gel electrophoresis, a *Pst*I digest of bovine genomic DNA formed two major spots, each comprised of ~700 bp fragments (Fig. 2). These were located separately from the 'arch' that was formed by the bulk of the genomic fragments. Their separate locations suggested that the repeating unit of the satellite I DNA consisted of two conformationally different DNA domains. We cloned the DNA fragments that were contained in these spots and analyzed their nucleotide sequences. For each spot, four clones were randomly selected and sequenced. It was revealed that the upstream half of the satellite I repeating unit formed spot F (named for fast) and the rest of the region formed spot N (for normal). The clones were named fragments F (the spot F-comprising fragment) and N (the spot N-comprising fragment). Figure 3 shows their nucleotide sequences. Fragments F and N showed 93 and 97% homology, respectively, to the corresponding regions of the reported satellite I DNA sequence (16). As indicated in Figure 3, we found a predominance (>80%) of purine–purine (or pyrimidine–pyrimidine) base stacking over purine–pyrimidine (or pyrimidine–purine) throughout the entire satellite I sequence. Furthermore, it contained a great many runs of three or more consecutive purine (or pyrimidine) residues.

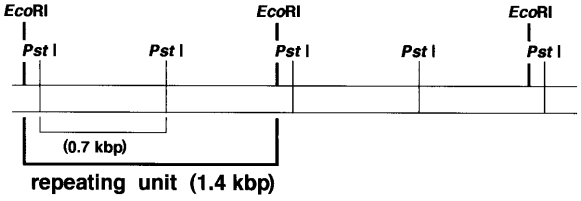

Figure 1. Positions of two *Pst*I sites in the repeating unit of bovine satellite I DNA.

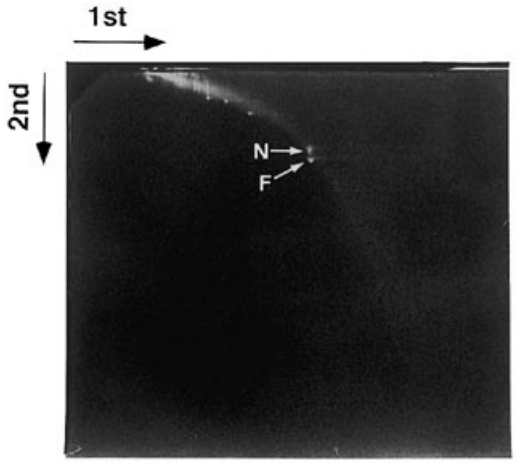

Figure 2. 2D gel electrophoresis of a digest of bovine genomic DNA with *Pst*I. The DNA fragments contained in spots F and N were extracted and cloned for further analyses.

One half of the repeating unit showed unusually rapid migration at low temperature

The electrophoretic behaviors of the F and N fragments were analyzed under various conditions. Initially, temperature-dependent changes in their mobilities were investigated by using 7.5% non-denaturing polyacrylamide gels. Fragment F showed unusually rapid migration at low temperature (Fig. 4A). Its relative size (Rs = apparent size/actual size; the size in bp is the total number of bp, which does not include single-stranded ends in this study) was ~0.9 at 5°C. The anomaly was pronounced at low temperature, but disappeared at 50°C. This phenomenon was similar to that observed for many curved DNAs in that unusual behavior is more pronounced at low temperature. However, curved DNAs migrate unusually slowly in non-denaturing polyacrylamide gels (14,17–21). On the other hand, the Rs values of the N fragment were almost unchanged being ~1.00 over the temperature range examined.

Next, we investigated the relationship between polyacrylamide concentration in gels and electrophoretic behavior (Fig. 4B). In this experiment, which was carried out at 5°C, the Rs values of the N fragment changed in a polyacrylamide-concentration-dependent manner. The values gradually rose from ~0.99 to ~1.06 as the concentration was raised. This phenomenon was reminiscent of the behaviors of curved DNA fragments. The extent of the unusual behavior observed for curved DNAs (retarded migration in this case) usually depends on polyacrylamide concentration in gels and increases as the concentration is raised (19). The Rs values of the fragment F also slightly changed according to the change in polyacrylamide concentration in gels. Although the relationship between the Rs value and the polyacrylamide concentration was not very clear for this case, the electrophoretic anomaly of the fragment was slightly more pronounced in 15% gels.

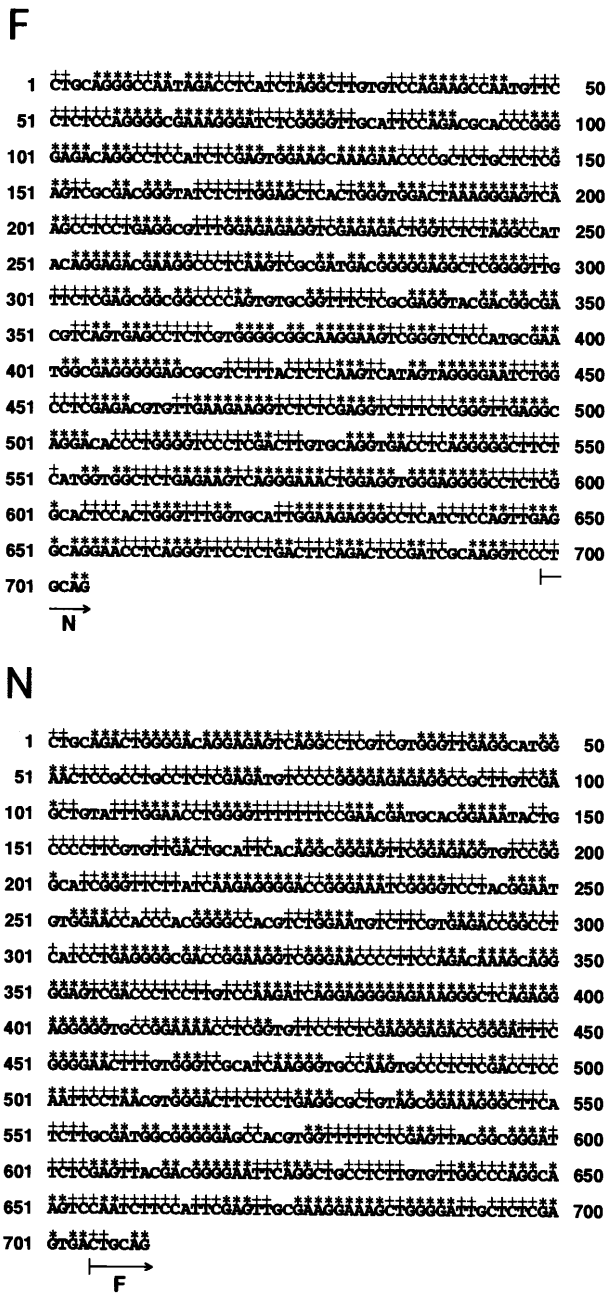

Figure 3. Nucleotide sequences of F and N fragments. *Pst*I sites located at both ends of F and N fragments are numbered in each fragment. Runs of consecutive purine or pyrimidine residues (including dinucleotides) are marked with * and +, respectively.

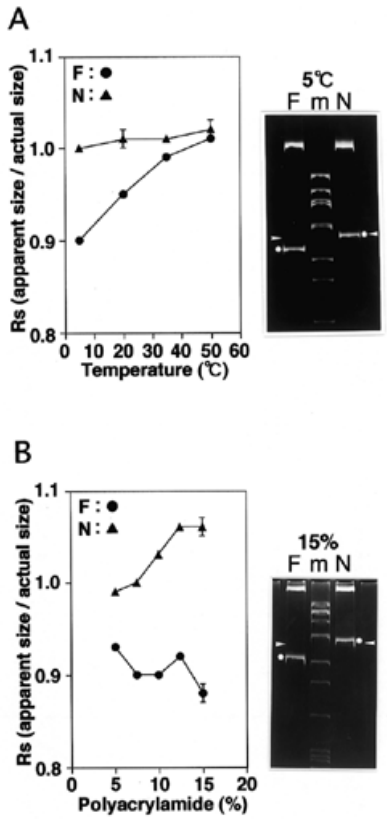

Figure 4. Temperature- or polyacrylamide-concentration-dependent changes in electrophoretic behavior of fragments F and N. (**A**) Temperature-dependent changes in electrophoretic behavior of the fragments F (●) and N (▲). Electrophoreses were carried out at 5, 20, 35 and 50°C by using 7.5% gels as described in Materials and Methods. The Rs means the ratio of the apparent size to the actual size. The values represent mean (± SD) of triplicate determinations. An example of the electrophoretic behaviors of these fragments, obtained at 5°C, is shown at the right. The bands formed by fragments F and N are indicated by white asterisks and the expected mobilities of these fragments are indicated by white arrowheads. Lane m, a marker; mixture of *Hin*cII digest of phage ϕX174 DNA and *Hae*III digest of the DNA. (**B**) Polyacrylamide-concentration-dependent changes in electrophoretic behavior of the fragments F (●) and N (▲). The electrophoreses were carried out at 5°C by using 5, 7.5, 10, 12.5 and 15% gels. Values represent mean (± SD) of triplicate determinations. An example of the electrophoretic behaviors of these fragments in a 15% gel is shown at the right.

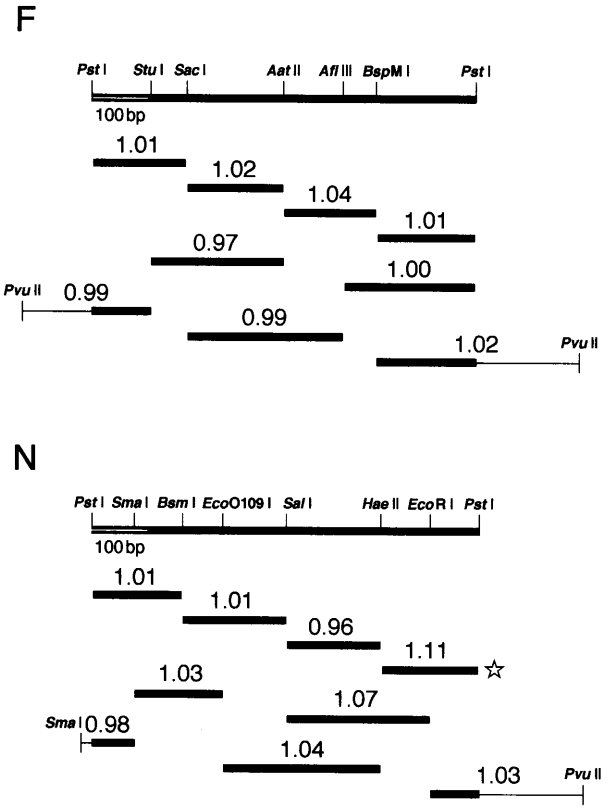

Figure 5. Mapping of the locus responsible for the rapid migration. Electrophoresis of F- and N-derived restriction fragments, which are indicated by straight bold lines below restriction maps of fragments F and N, was carried out at 5°C by using a 7.5% non-denaturing polyacrylamide gel. The relative sizes of the restriction fragments are shown above the corresponding bold lines. Thin horizontal lines attached to several bold lines indicate pUC19 DNA. Scale bars of 100 bp are indicated within the top bold lines indicating F and N fragments. The fragment marked with a star was used for circular permutation analysis (Fig. 6).

Bent DNA exists in the repeating unit

The F and N fragments were digested with several restriction enzymes as indicated in Figure 5 and electrophoretic behaviors of the resulting fragments were further studied. Several restriction fragments migrated slightly faster than expected, such as F-derived *Stu*I–*Aat*II and *Sac*I–*Afl*III fragments and N-derived *Sal*I–*Hae*II fragments. However, it was unexpected that many fragments showed almost normal mobilities. Very interestingly, N-derived *Hae*II–*Pst*I and *Sal*I–*Eco*RI fragments showed noticeable retarded migration that is characteristic of curved DNA fragments. Judging from the result that the Rs value of *Sal*I–*Hae*II fragment was low, the same curvature which was contained in the *Hae*II–*Eco*RI region seemed to have retarded mobilities of the *Hae*II–*Pst*I and *Sal*I–*Eco*RI fragments. Heretofore, the rapid migration property of the satellite I DNA seems to have concealed the presence of the curved DNA structure.

The center of the intrinsic DNA curvature located in the *Hae*II–*Pst*I region of the N fragment was analyzed by using circular permutation analysis. The center was revealed to be located approximately between positions 600 and 610 (Fig. 6). The nucleotide sequence between positions 570 and 640 contained periodically spaced $(T)_{2–5}$ tracts, which seem to be the determinants of the intrinsic DNA curvature.

Metal ions retarded mobility of the F fragment

DNA interacts with divalent cations and conformations of several DNAs are influenced by their presence (22–29). It was of interest to know whether conformations of F and N fragments were affected by Mg^{2+} and Ca^{2+} ions. Thus, we carried out circular permutation analyses in the presence of these ions (Fig. 7). As the *Pst*I ends of both fragments were found to influence their mobilities in the electrophoretic condition containing Mg^{2+} or Ca^{2+} ions (presumably by intramolecular interaction; not shown), we employed blunt-ended fragments in this experiment (we made all fragments carry blunt ends). As shown in Figure 7, every F-derived permuted fragments showed larger Rs values (some of

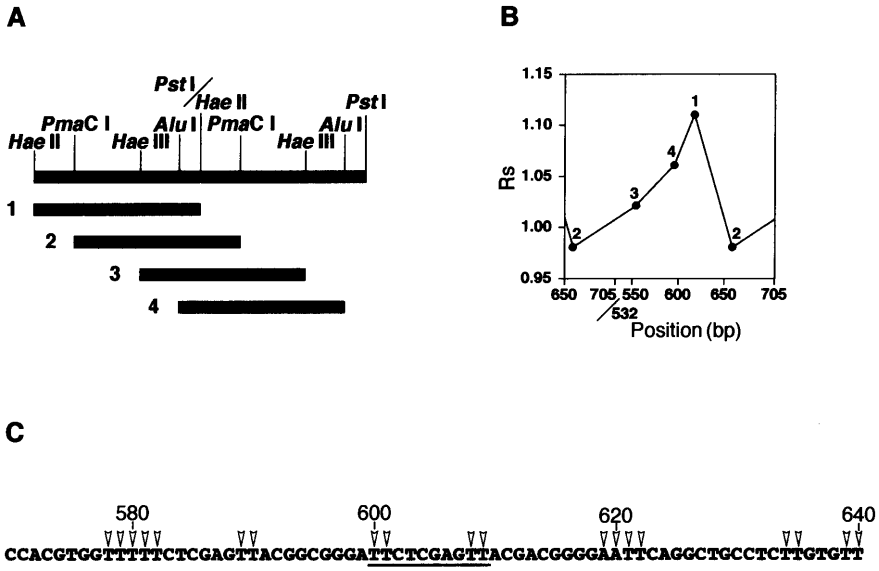

Figure 6. Mapping of the locus of an intrinsic DNA curvature in *Hae*II–*Pst*I region of the N fragment. (**A**) Circularly permuted fragments used for the analysis. Fragments 2, 3 and 4 were generated by digesting the tandem dimer of the *Hae*II–*Pst*I fragment with *Pma*CI, *Hae*III and *Alu*I, respectively, and fragment 1 was obtained directly from N fragment. (**B**) Mapping of the curved center. Nucleotide sequence position is numbered from the first base pair present on the *Pst*I site located at the 5′-end of N fragment. Relative sizes of the permuted fragments are plotted against the center positions of the respective fragments. (**C**) Nucleotide sequence including the center region of the curvature. The curved center is underlined. Arrowheads indicate $(T)_{2–5}$ and $(A)_2$ tracts.

them were >1.0) in the presence of the divalent cations when compared with the data points obtained in the absence of them, and among the elevated Rs values a peak value was observed in the respective plots, indicating that a wide region of the F fragment formed a slightly curved DNA conformation in the solution containing Mg^{2+} or Ca^{2+} ions. Ca^{2+} ions generated a slightly larger effect than Mg^{2+} ions. The figure indicated that the center region of each induced DNA bend was located approximately between positions 1 and 100. However, we could not identify any distinctive feature within the locus.

The N-derived fragments gave almost the same results irrespective of the difference in electrophoretic condition. The pattern of data points obtained in the absence of the divalent cations indicated that the region spanning from position ~350 to ~700 of N fragment formed an intrinsic DNA curvature. The shape of this curvature seemed to be retained in the solution containing Mg^{2+} or Ca^{2+} ions. This region includes a curved DNA structure that was identified in Figure 6. Furthermore, we find $(A/T)_{2–3}$ tracts at positions 335–336, 343–345, 365–366 and 387–389 in DNA sequence of the N fragment (Fig. 3). They may also form a small curvature. The Rs value 1.04 of N-derived *Eco*O109I–*Hae*II fragment (Fig. 5) suggests this possibility.

DISCUSSION

In order to obtain some clue to understanding the molecular mechanism behind the rapid migration behavior of DNA fragments, the physical properties of bovine satellite I DNA were analyzed in detail by using polyacrylamide gel electrophoreses. The F fragment showed temperature-dependent increased mobility in non-denaturing polyacrylamide gels in the absence of metal ions (Fig. 4A). It showed greatly increased mobilities at low temperature, while it behaved normally at high temperature. This phenomenon is just the opposite but, in a sense, very similar to those shown by curved DNA fragments. The N fragment did not show such a temperature-dependent electrophoretic anomaly (Fig. 4A) although it contained a curved DNA structure (Fig. 6). It is logical to assume that the phenomenon of retarded migration caused by the DNA curvature occurring in the N fragment was suppressed by rapid migration property of the fragment. The result shown in Figure 7 seems to support this interpretation. The rapid migration property seems to have equally lowered Rs values of all N-derived permuted fragments. We can also understand the result shown in Figure 4B in the same way. Reduced mobilities of curved DNA fragments are known to be more pronounced in gels with high polyacrylamide concentration (19). This effect seemed to predominate over the rapid migration property of the N fragment in 10–15% gels. On the other hand, the rapid migration property dominated slightly in 5% gels presumably because the effect of curved DNA structure was small under that condition. In conclusion, both of the F and N fragments, in other words, the whole region of the satellite I repeating unit has a property that drives the unit to move unusually rapidly in non-denaturing polyacrylamide gels. The presence of an intrinsic DNA curvature in the N fragment seems to be the main difference between the F and N fragments, which seems to have resulted in the formation of two spots on the 2D gel (Fig. 2).

We found a predominance (>80%) of purine–purine base stacking over purine–pyrimidine throughout the entire satellite I sequence. Also, we found that the sequence contained a great many runs of three or more consecutive purine residues (Fig. 3). Purine stacking interactions are thought to provide most of the mechanical rigidity of the DNA helix (30). The rigidity of DNA may be the principal cause of the rapid migration. Stiff and rod-like molecules may exhibit minimal frictional drag as they pass through the tight pores of a polyacrylamide gel (11). Based on this interpretation, we can explain the temperature-dependent mobility change observed for the F fragment (Fig. 4A); i.e., it had

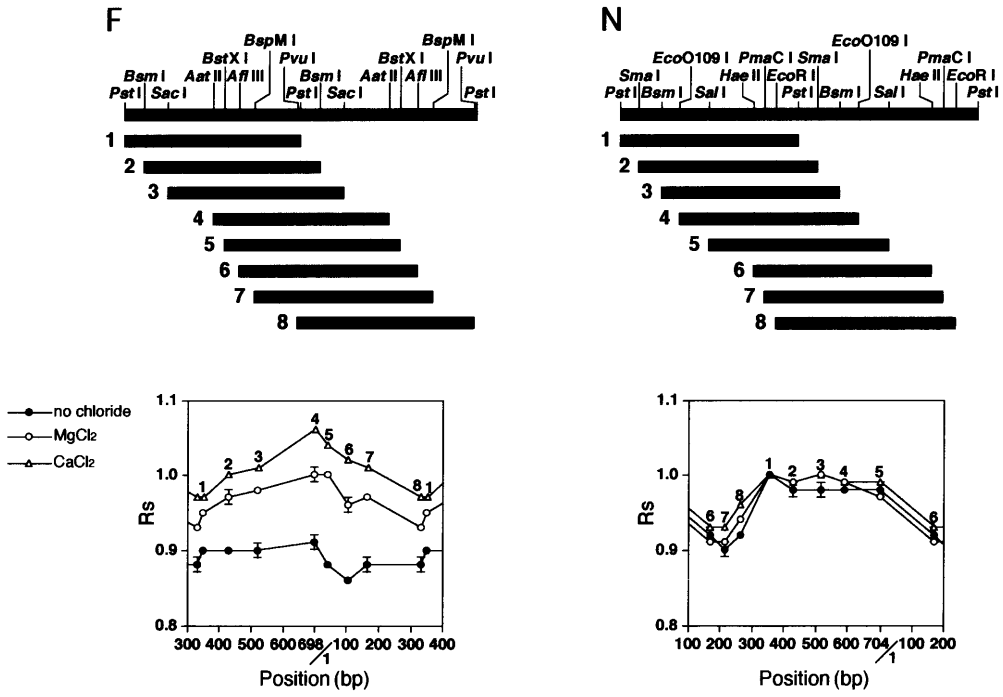

Figure 7. Effect of Mg^{2+} and Ca^{2+} ions on conformations of F and N fragments. F and N fragments were subjected to circular permutation analyses. Electrophoreses were carried out at 5°C in the presence of 10 mM $MgCl_2$ (○) or $CaCl_2$ (Δ), or in the absence of these chlorides (●). Relative sizes of the permuted fragments are plotted against the center positions of the respective fragments. The Rs values represent mean (± SD) of triplicate determinations.

'normal' flexibility at high temperature. How can we explain why many F-derived small segments did not show a large electrophoretic anomaly like that shown by the F fragment (Fig. 5)? It may be that electrophoretic detection of rigidity (or flexibility) of DNA molecules becomes difficult when their sizes become near persistence length of ~150–200 bp (for persistence length, see 31).

An alternative explanation, however, is still possible for rapid migration. Runs of consecutive purine DNA sequence are known to set up an A-like helix (25,32). The length of A-DNA is ~30% shorter than B-DNA of the same bp (helix parameters were from Dickerson *et al*; 33). Thus, it is possible to explain that the runs of three or more consecutive purine residues may make satellite I DNA adopt A-family-like DNA conformation (we are now examining this possibility) and unusually fast migration of the DNA may be caused by the reduced length. In this interpretation, we need not imagine a full-blown switch to A-form DNA because, for example, the F fragment would only need to be 90% of the length of 'ordinary' DNA in order to have an Rs value of 0.9. It may be that, on average, the unusually high proportion of purine–purine and pyrimidine–pyrimidine steps can reduce the 'rise' per dinucleotide step along the axis as a result of a combined effect of modest roll and slide. In any case, it seems safe to conclude that the scattered runs of consecutive purine DNA sequence are responsible for the rapid migration.

Mg^{2+} and Ca^{2+} ions reduced the electrophoretic mobility of F fragment (Fig. 7). We interpreted that the fragment was induced to be slightly bent. A very similar phenomenon was reported; i.e., Zn^{2+} ions induced a bend within a DNA that was also rich in runs of three or more consecutive purine residues (25). More interestingly, that DNA was thought to adopt A-DNA conformation. Considering that the F fragment contained a great many runs of three or more consecutive purine residues throughout its sequence, these runs are assumed to have responded to Mg^{2+} or Ca^{2+} ions. Mechanistically, asymmetric charge neutralization of the sugar–phosphate backbone, which can lead to curvature of the helix axis (26), might have occurred within the F fragment. To our knowledge, our result presented here is the first indication of Mg^{2+}- or Ca^{2+}-ion-induced bend of natural DNA. The curved conformation of N fragment was not affected by the divalent cations, though the fragment was also rich in consecutive purine tracts. This result indicates that Mg^{2+} and Ca^{2+} ions did not generate such a strong effect as changed extent of the intrinsic DNA curvature.

The argument for the universality of bent satellite DNA is strongly supported by the fact that bovine satellite I DNA also contained an intrinsic DNA curvature. Indeed, we also found a 'concealed' curvature in human α-satellite DNA (data not shown). Although we do not still deny the possibility of the existence of non-bent satellite DNA sequences, such sequences, if they exist, are likely to have some specific reason for adopting the non-bent structure. For example, they may substitute the metal-ion-induced DNA bend or protein-induced DNA bend for the intrinsically curved DNA structure. Chromatin appears as a 'beads-on-a-string' configuration at a very low salt condition, while it condenses to form irregular rod-like structures with a diameter of ~30 nm at moderate ionic strengths (34–36). Intrinsic DNA curvatures and the induced DNA bends may play different roles in the folding of satellite I DNA; e.g., the former may function in the formation of periodically spaced nucleosomal arrays and the latter in completing higher-order organization of the nucleosomal arrays.

ACKNOWLEDGEMENTS

We wish to thank Junko Ohyama for help in preparing the manuscript. This study was partly supported by a Grant-in-Aid for Scientific Research (No. 09680681) from the Ministry of Education, Science, Sports and Culture of Japan to T.O.

REFERENCES

1 John,B. and Miklos,G.L.G. (1979) *Int. Rev. Cytol.*, **58**, 1–114.
2 Singer,M.F. (1982) *Int. Rev. Cytol.*, **76**, 67–112.
3 Trifonov,E.N. and Sussman,J.L. (1980) *Proc. Natl Acad. Sci. USA*, **77**, 3816–3820.
4 Drew,H.R. and Travers,A.A. (1985) *J. Mol. Biol.*, **186**, 773–790.
5 Wada-Kiyama,Y. and Kiyama,R. (1996) *Mol. Cell. Biol.*, **16**, 5664–5673.
6 Radic,M.Z., Lundgren,K. and Hamkalo,B.A. (1987) *Cell*, **50**, 1101–1108.
7 Kodama,H., Saitoh,H., Tone,M., Kuhara,S., Sakaki,Y. and Mizuno,S. (1987) *Chromosoma*, **96**, 18–25.
8 Benfante,R., Landsberger,N., Tubiello,G. and Badaracco,G. (1989) *Nucleic Acids Res.*, **17**, 8273–8282.
9 Martínez-Balbás,A., Rodríguez-Campos,A., García-Ramírez,M., Sainz,J., Carrera,P., Aymamí,J. and Azorín,F. (1990) *Biochemistry*, **29**, 2342–2348.
10 Fitzgerald,D.J., Dryden,G.L., Bronson,E.C., Williams,J.S. and Anderson,J.N. (1994) *J. Biol. Chem.*, **269**, 21303–21314.
11 Anderson,J.N. (1986) *Nucleic Acids Res.*, **14**, 8513–8533.
12 Milot,E., Belmaaza,A., Wallenburg,J.C., Gusew,N., Bradley,W.E.C. and Chartrand,P. (1992) *EMBO J.*, **11**, 5063–5070.
13 Ohyama,T. and Kusakabe,T. (1993) *Anal. Biochem.*, **212**, 287–289.
14 Wu,H.M. and Crothers,D.M. (1984) *Nature*, **308**, 509–513.
15 Kurnit,D.M., Shafit,B.R. and Maio,J.J. (1973) *J. Mol. Biol.*, **81**, 273–284.
16 Plucienniczak,A., Skowronski,J. and Jaworski,J. (1982) *J. Mol. Biol.*, **158**, 293–304.
17 Diekmann,S. (1987) *Nucleic Acids Res.*, **15**, 247–265.
18 Ohyama,T. (1996) *J. Biol. Chem.*, **271**, 27823–27828.
19 Marini,J.C., Levene,S.D., Crothers,D.M. and Englund,P.T. (1982) *Proc. Natl Acad. Sci. USA*, **79**, 7664–7668.
20 Calladine,C.R., Drew,H.R. and McCall,M.J. (1988) *J. Mol. Biol.*, **201**, 127–137.
21 Hagerman,P.J. (1990) *Annu. Rev. Biochem.*, **59**, 755–781.
22 Daune,M. (1974) In Sigel,H. (ed.), *Metal Ions in Biological Systems: Vol. 3, High Molecular Weight Complexes*. Marcel Dekker, NY, pp. 1–43.
23 Eichhorn,G.L. (1981) *Advan. Inorg. Chem.*, **3**, 1–46.
24 Cowan,J.A. (1995) In Cowan,J.A. (ed.), *The Biological Chemistry of Magnesium*. VCH Publishers, Inc., NY, pp. 185–209.
25 Nickol,J. and Rau,D.C. (1992) *J. Mol. Biol.*, **228**, 1115–1123.
26 Strauss,J.K. and Maher,L.J.,III (1994) *Science*, **266**, 1829–1834.
27 Brukner,I., Susic,S., Dlakic,M., Savic,A. and Pongor,S. (1994) *J. Mol. Biol.*, **236**, 26–32.
28 Dlakic,M. and Harrington,R.E. (1996) *Proc. Natl Acad. Sci. USA*, **93**, 3847–3852.
29 Han,W., Lindsay,S.M., Dlakic,M. and Harrington,R.E. (1997) *Nature*, **386**, 563.
30 Hagerman,K.R. and Hagerman,P.J. (1996) *J. Mol. Biol.*, **260**, 207–223.
31 Hagerman,P.J. (1988) *Annu. Rev. Biophys. Biophys. Chem.*, **17**, 265–286.
32 Fairall,L., Martin,S. and Rhodes,D. (1989) *EMBO J.*, **8**, 1809–1817.
33 Dickerson,R.E., Drew,H.R., Conner,B.N., Kopka,M.L. and Pjura,P.E. (1983) *Cold Spring Harbor Symp. Quant. Biol.*, **47**, 13–24.
34 Thoma,F., Koller,T. and Klug,A. (1979) *J. Cell Biol.*, **83**, 403–427.
35 Wolffe,A. (1995) *Chromatin: Structure and Function*. 2nd ed., Academic Press, London.
36 Leuba,S.H., Yang,G., Robert,C., Samori,B., van Holde,K., Zlatanova,J. and Bustamante,C. (1994) *Proc. Natl Acad. Sci. USA*, **91**, 11621–11625.